ОБЪЕДИНЕННЫЙ
ИНСТИТУТ
ЯДЕРНЫХ
ИССЛЕДОВАНИЙ
ДУБНА

E17 - 9354

E.Kolley, W.Kolley

EFFECT OF THERMAL FLUCTUATIONS ON THE ELECTRONIC DENSITY OF STATES IN DISORDERED BINARY ALLOYS

II. Numerical Results

1975

E17 - 9354

E.Kolley, W.Kolley

EFFECT OF THERMAL FLUCTUATIONS ON THE ELECTRONIC DENSITY OF STATES IN DISORDERED BINARY ALLOYS

II. Numerical Results

Submitted to physica status solidi

1. INTRODUCTION

In Part I [1] the model Hamiltonian

$$H = \sum_{n} (\epsilon_n + \Theta_{nn}) a_n^+ a_n + \sum_{\substack{n,m \\ (m \neq n : n.n.)}} (h_{nm} + \Theta_{nm}) a_n^+ a_m, \quad (1)$$

with

$$\Theta_{nm} = \sum_{s} (\gamma_{nm}^{(s)} b_s + (\gamma_{mn}^{(s)})^* b_s^+), \quad (2)$$

has been proposed to study the electronic properties of disordered binary alloys $A_c B_{1-c}$ in the presence of electron-phonon interaction. $a_n^+ (a_n)$ and $b_s^+ (b_s)$ are the creation (annihilation) operators for an electron in the Wannier state at lattice site n and for a phonon in the state with the quantum number s, respectively. The atomic energies ϵ_n, the hopping integrals h_{nm}, the electron-phonon coupling elements $\gamma_{nn}^{(s)}$ and $\gamma_{nm}^{(s)}$ are random variables which take the values ϵ^ν, $h^{\nu\mu}$, $\gamma^{(s)\nu}$ and $\gamma^{(s)\nu\mu}$ ($\nu, \mu = A, B$), respectively, according to whether an A or B atom occupies the site n (the nearest-neighbour site m).

This model describes a combined effect of disorder. The coupling of electronic states with lattice vibrations leads to the modulation (thermal fluctuations) of the substitutionally random potentials. The off-diagonal randomness was specialized in Part I by assuming the additive conditions

$$h^{AB} = \frac{1}{2}(h^{AA} + h^{BB}), \qquad (3)$$

$$\gamma^{(s)AB} = \frac{1}{2}(\gamma^{(s)AA} + \gamma^{(s)BB}). \qquad (4)$$

For comparison, two special cases of the model Hamiltonian (1) are pointed out. In the absence of off-diagonal randomness, this model was investigated by Chen et al. [2]. The case without electron-phonon interaction (i.e., the static-alloy limit) has been recently studied by Fukuyama et al. [3] under the condition (3) (cf. also [4]). The theories developed for those specialized models are based on the coherent potential approximation (CPA).

In the present paper we analyse numarically the CPA equations for the electronic self-energy derived in Part I.

2. BASIC RELATIONS

In this section some relations from Part I are summarized. Using (3) and (4) the Hamiltonian (1) may be rewritten as

$$H = H_e^B + \sum_n V_n . \qquad (5)$$

H_e^B is the one-electron Hamiltonian for a perfect B crystal; the random part V_n including off-diagonal disorder denotes the perturbation related to the site n.

The averaged one-electron Green's function in Bloch representation

$$\mathcal{G}_{\vec{k}}(z) = \langle\langle (z-H)^{-1} \rangle_{ph} \rangle_{c;\vec{k}} = (z - \epsilon^B - h^{BB} s(\vec{k}) - \Sigma(z,\vec{k}))^{-1}, \qquad (6)$$

with

$$s(\vec{k}) = \sum_{m \neq n:\, n.n.} e^{i\vec{k}(\vec{R}_m - \vec{R}_n)}, \qquad (7)$$

is related to interesting macroscopic properties of the system. $\langle \ldots \rangle_{ph}$ means the thermal average over all phonon states in a given alloy configurations; $\langle \ldots \rangle_c$ denotes the configuration average. Here the adiabatic approximation was used in order to perform two independent procedures of averaging successively.

The electronic self-energy $\Sigma(\vec{k}, z)$ corresponding to the random additive operator $\sum_n V_n$ can be calculated within the single-site CPA.

The momentum-dependent self-energy

$$\Sigma(\vec{k}, z) = \sigma_0(z) + 2\sigma_1(z)s(\vec{k}) + \sigma_2(z)s^2(\vec{k}) \qquad (8)$$

is expressed in terms of σ_0, σ_1, σ_2 satisfying the CPA equations

$$\iint_{-\infty}^{+\infty} d\eta\, d\zeta\, e^{-(\eta^2+\zeta^2)} \Big\{ c \frac{a_\ell(z; \epsilon^A - \epsilon^B, \frac{1}{2}(h^{AA} - h^{BB}); \sqrt{2a^A}\eta, \sqrt{2\delta^A}\zeta)}{1 - D(z; \epsilon^A - \epsilon^B, \frac{1}{2}(h^{AA} - h^{BB}); \sqrt{2a^A}\eta, \sqrt{2\delta^A}\zeta)} +$$

$$+ (1-c) \frac{a_\ell(z; 0, 0; \sqrt{2a^B}\eta, \sqrt{2\delta^B}\zeta)}{1 - D(z; 0, 0; \sqrt{2a^B}\eta, \sqrt{2\delta^B}\zeta)} \Big\} = 0, \qquad (9)$$

where

$$a_0(z; \epsilon, h; \eta, \zeta) = (\epsilon + \eta - \sigma_0) + (h + \zeta - \sigma_1)^2 F_2 + (\epsilon + \eta - \sigma_0)\sigma_2 F_2, \qquad (10)$$

$$a_1(z; \epsilon, h; \eta, \zeta) = (h + \zeta - \sigma_1) - (h + \zeta - \sigma_1)^2 F_1 - (\epsilon + \eta - \sigma_0)\sigma_2 F_1, \qquad (11)$$

$$a_2(z; \epsilon, h; \eta, \zeta) = -\sigma_2 + (h + \zeta - \sigma_1)^2 F_0 + (\epsilon + \eta - \sigma_0)\sigma_2 F_0, \qquad (12)$$

$$D(z; \epsilon, h; \eta, \zeta) = (\epsilon + \eta - \sigma_0)F_0 + 2(h + \zeta - \sigma_1)F_1 - \sigma_2 F_2 - \qquad (13)$$

$$- [(h + \zeta - \sigma_1)^2 + (\epsilon + \eta - \sigma_0)\sigma_2][F_1^2 - F_0 F_2],$$

$$F_\ell(z) = \frac{1}{N}\sum_{\vec{k}} \mathcal{G}_{\vec{k}}(z)[s(\vec{k})]^\ell, \qquad (\ell = 0, 1, 2). \qquad (14)$$

The parameters a^ν and δ^ν characterize thermal fluctuations of the atomic energies and the hopping integrals, respectively. Their temperature T dependence was found as

$$a^\nu = \langle \sum_s | \gamma^{(s)\nu} |^2 \coth\left(\frac{h\omega_s}{2kT}\right) \rangle_c^{|\nu}, \qquad (15)$$

$$\delta^\nu = \frac{1}{4} \langle \sum_s | \gamma^{(s)\nu\nu} |^2 \coth\left(\frac{h\omega_s}{2kT}\right) \rangle_c^{|\nu}, \quad (\nu = A, B). \qquad (16)$$

Here ω_s are the phonon frequencies in a particular alloy configurations; $\langle \ldots \rangle_c^{|\nu}$ denotes the average over all configurations with the fixed ν-atom at a single site.

Using Hubbard's semielliptic form /5/ for the unperturbed density of states (related to H_e^B), the coherent Green's functions $F_\ell(z)$ (14) can be expressed analytically in terms of σ_0, σ_1, σ_2 (see Part I).

3. NUMERICAL RESULTS AND DISCUSSION

The set of coupled equations (9) for $\sigma_0(z)$, $\sigma_1(z)$, $\sigma_2(z)$ is self-consistently solved by using a generalization /6/ of the iterative average-t-matrix approximation (IATA) suggested by Chen /7/. In our case the generalized iterative procedure is applied to a system of integral equations. For each step of iteration, the double integration in (9) is carried out numerically by a two-dimensional Hermite integration /8/. Starting from the values of the self-energy in the virtual-crystal approximation, we get fast convergence for most cases. The knowledge of σ_0, σ_1, σ_2 allows one to determine the electronic density of states per atom through

$$\rho(E) = -\frac{1}{\pi} \mathrm{Im}\, F_0(E + i0). \qquad (17)$$

Let us summarize the imput quantities for the computation. We can vary the concentration c of A atoms, the thermal fluctuation parameters a^A, a^B, δ^A, δ^B (proportional to T at high temperatures), the parameters Δ_0 and Δ_1 defined by

$$\Delta_0 = \epsilon^A, \quad \Delta_1 = 6(h^{AA} - h^{BB}), \qquad (18)$$

which describe diagonal and off-diagonal randomness, respectively. The quantity h^{BB} is fixed in the case of the simple cubic lattice as $h^{BB} = \frac{1}{6}$; the energy ϵ^B is chosen equal to zero. As has been mentioned in estimating the fluctuation parameters in Part I, the values of a^ν and δ^ν will be chosen without definite assumptions about ω_s, , $\gamma^{(s)\nu}$ and $\gamma^{(s)\nu\nu}$. Note that if the electron-phonon interaction is assumed to be independent of configurational disorder, then the following identities hold:

$$a = a^A = a^B, \quad \delta = \delta^A = \delta^B. \qquad (19)$$

In this section we present numerical results for the density of states and the self-energy as functions of energy for various alloy parameters including electron-phonon correlations. Some features of this model calculation are pointed out.

The density of states in the static limit (i.e., $a = 0, \delta = 0$) is shown in Fig. 1. Two impurity-scattering mechanisms associated with Δ_0 and Δ_1 are taken into account. Formally, the scattering of the electron arises from nonlocalized perturbations

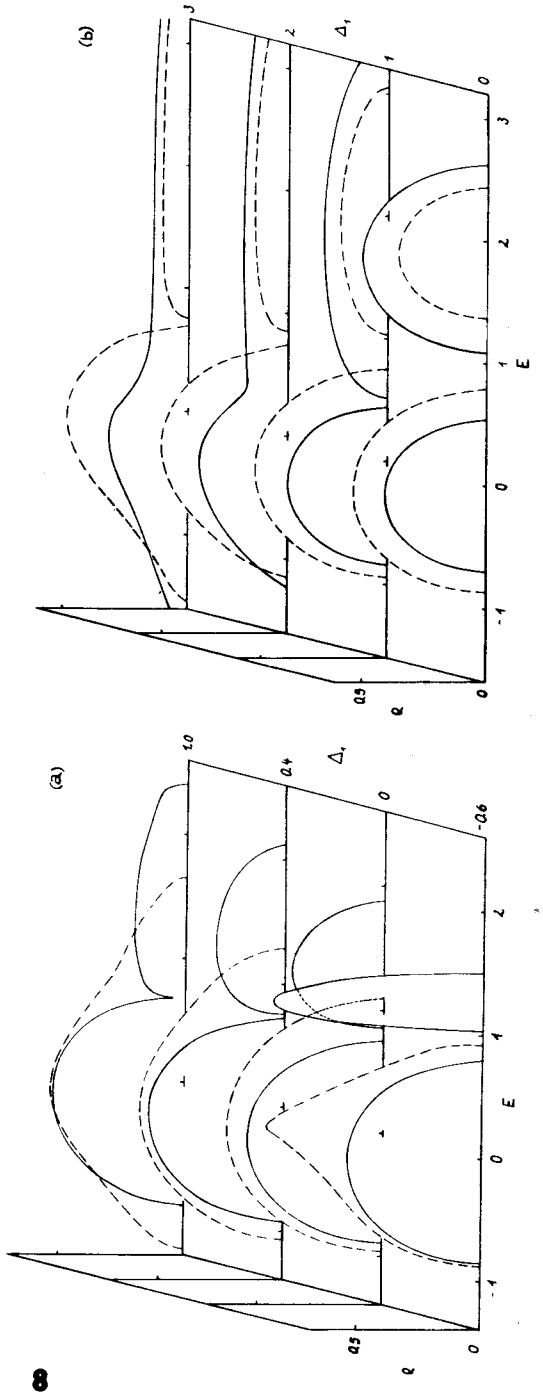

Fig. 1. Electronic density of states $\rho(E)$ at various values of the off-diagonal randomness parameter Δ_1 for static alloys ($\alpha = 0$, $\delta \neq 0$) with (a) $c = 0.3$, , $\Delta_0 = 1.2$ (full lines) and $\Delta_0 = 0.2$ (dashed lines); and (b) $\Delta_0 = 1.8$, $c = 0.6$ (full lines) and $c = 0.3$ (dashed lines).

introduced by substituting A atoms for B atoms. For weak scattering related to $\Delta_0 = 0.2$ (Fig. 1(a)), the continuous band is stretched with increasing Δ_1. Starting from the split-band case ($\Delta_0 > 1$, small Δ_1), the energy gap between the two subbands disappears when Δ_1 increases (Fig. 1 (a) and (b)). The extreme bandwidths are produced by dominant off-diagonal scattering for large values of the hopping integral between A and B atoms. In the opposite limit ($\Delta_1 < 0$), the narrowing of the minority subband is due to the fact that here the hopping within the A component is visibly diminished.

Fig. 2 shows the temperature dependence of the density of states for an alloy in the split-band regime caused by diagonal disorder only. Corresponding to the numerical

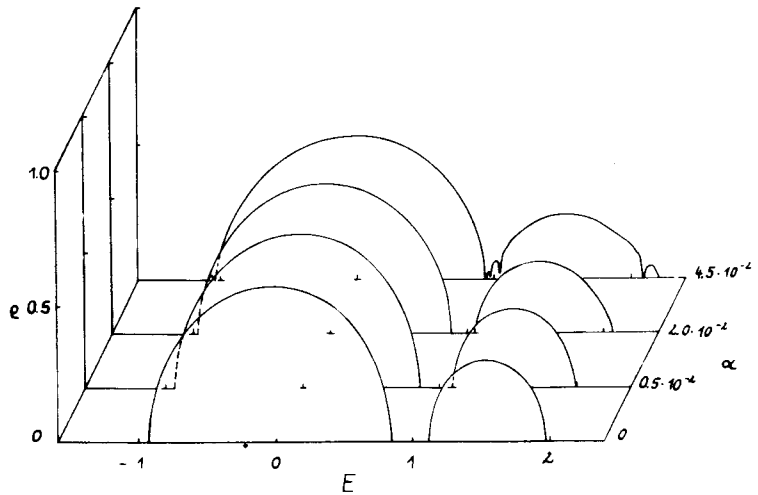

Fig. 2. Electronic density of states $\rho(E)$ in the case of purely diagonal scattering ($\Delta_1 = 0$, $\delta = 0$) at several temperatures characterized by different α values for an alloy with $c = 0.2$, $\Delta_0 = 1.4$.

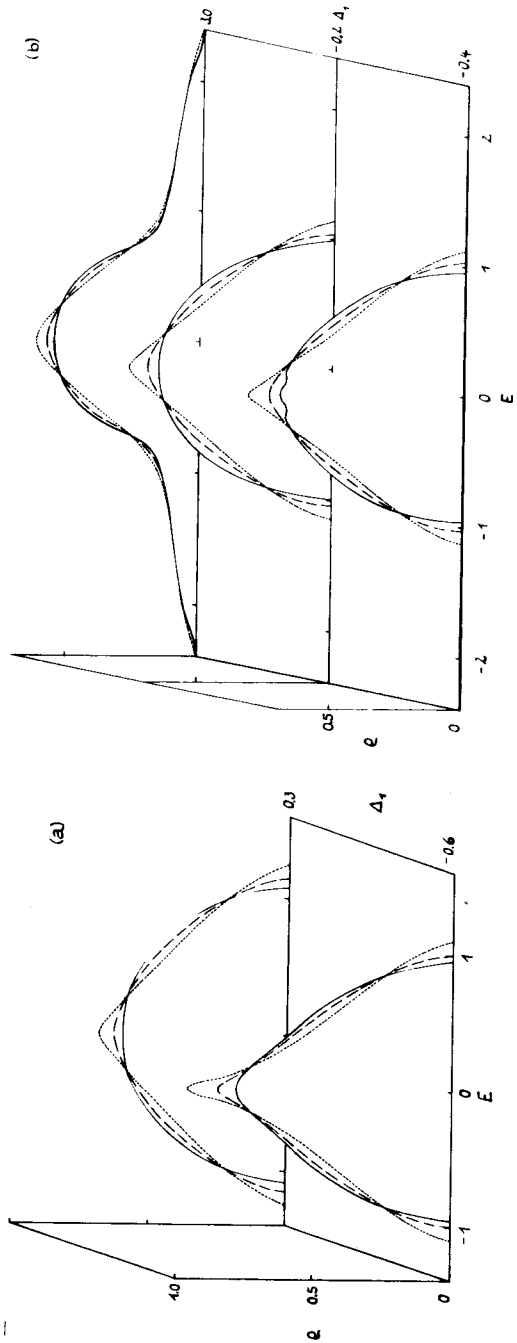

Fig. 3. Electronic density of states $\rho(E)$ in the case of purely off-diagonal scattering ($\Delta_0 = 0$, $\alpha = 0$) for various Δ_1 values. The figures represent alloys with (a) $c = 0.2$ and (b) $c = 0.15$ at several temperatures characterized by $\delta = 0$ (full lines), $\delta = 4 \cdot 10^{-4}$ (dashed lines), and $\delta = 10^{-3}$ (dotted lines).

results of Chen et al.[2], the thermal fluctuations can close the band gap. Moreover, it should be noted that increasing potential fluctuations (here for $\alpha = 0.045$) give rise to fine structure near the edges of the minority subband. Such a situation is discussed in connection with Fig. 4.

The density of states in the case of purely off-diagonal scattering is presented in Fig. 3. In the static limit, this case was numerically studied by Fukuyama et al.[3]. Thermal fluctuations of the hopping integrals are reflected by the tendency to enhance the band maximum and broaden the static-alloy band. In the case $\Delta_1 = 3$ (Fig. 3 (b)) where the impurity scattering is most effective, the line shape is weakly modified with increasing δ, whereas the two broad tails of the band (compare [3]) are not affected by thermal disorder.

The curves in Fig. 4 illustrate the influence of thermal fluctuations characterized by the parameter pairs (α,δ) on the density of states. The change of $\rho(E)$ due to thermal disorder depends on the scattering character of the static alloy. In the unsplit-band case (Fig. 4(a)), increasing values of (α,δ) tend to stretch the band. Roughly speaking, the gaps in the split-band alloys (Fig. 4(b),(c),(d)) decrease gradually or vanish with increasing temperature. On the other hand, the thermal fluctuations can produce fine structure of a symmetric form in the region of the impurity subband. This effect is sensitive to the changes of (α,δ) and Δ_1 as shown in Fig. 4 (b), (c), (d). The fine structure appears in those cases where the average

Fig. 4. Electronic density of states $\rho(E)$ in the case of both diagonal and off-diagonal scattering with thermal disorder included. The alloy parameters are (a) $c = 0.4$, $\Delta_0 = 0.4$, $\Delta_1 = -0.5$; (b) $c = 0.2$, $\Delta_0 = 1.4$, $\Delta_1 = -0.6$; (c) $c = 0.2$, $\Delta_0 = 1.4$ with $\alpha = 0$, $\delta = 0$ (full lines), $\alpha = 2 \cdot 10^{-2}$, $\delta = 4 \cdot 10^{-5}$ (dashed lines), and $\alpha = 4.5 \cdot 10^{-2}$, $\delta = 10^{-4}$ (dotted lines); and (d) $c = 0.3$, $\Delta_0 = 1.2$ with $\alpha = 0$, $\delta = 0$ (full lines), $\alpha = 10^{-2}$, $\delta = 2 \cdot 10^{-5}$ (dashed lines), and $\alpha = 10^{-1}$, $\delta = 2 \cdot 10^{-4}$ (dotted lines). Different values of (α, δ) -pairs characterize several temperatures.

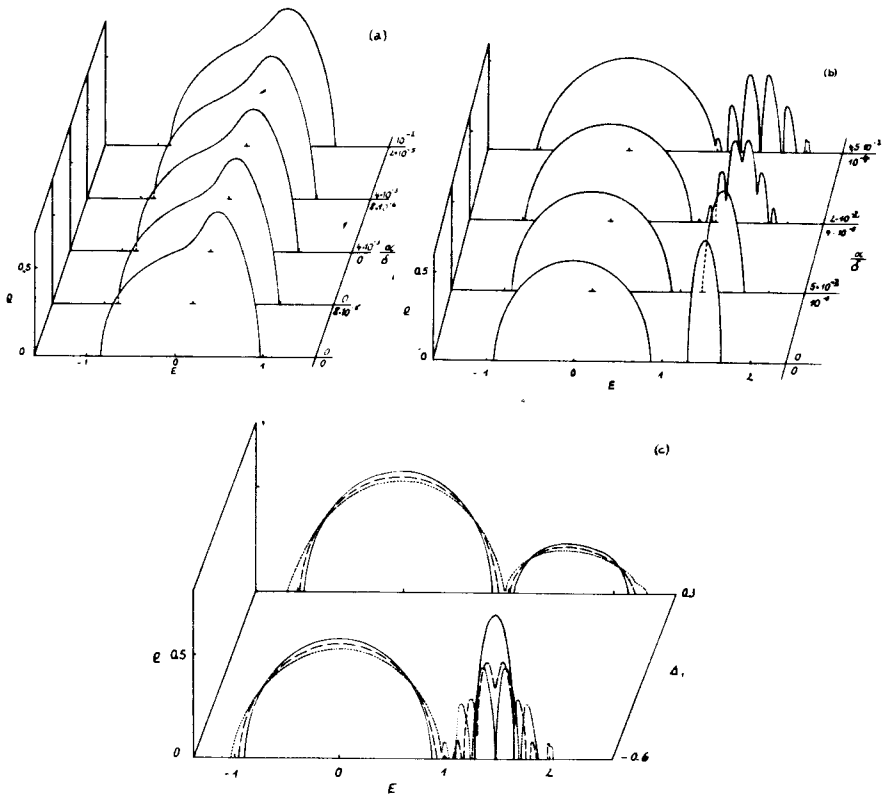

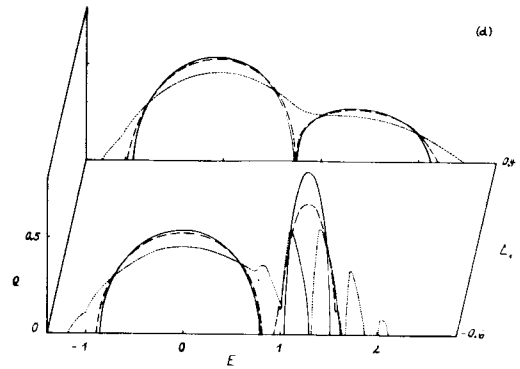

amplitude of the local potential fluctuation (i.e., the quantity $\sqrt{\alpha}$) attains the order of the half-band width of the minority subband corresponding to the static limit. A more detailed peaky structure in the spectrum is visible if we take larger values of (α, δ); here the value of $\sqrt{\alpha}$ exceeds the half-band width of the static-alloy minority subband. The pronounced structure, as expected, disappears with the increase of the bandwidth for the A component (i.e., for the transition from $\Delta_1 < 0$ to $\Delta_1 > 0$ in Fig. 4 (c), (d)). In the case of the main band, the thermal fluctuations are averaged out; tails and modified shapes of the state density are produced with increasing temperature.

More physically, the concept of the electron trapped by local (or nonlocal) lattice deformations due to lattice vibrations can be used to describe the effect of electron-phonon scattering. The situation is analogous to the impurity scattering in the random lattice where the electron is bound by impurity centres. The peaky structure and the satellites in the region of

the impurity subband (Fig. 4 (b), (c), (d)) can be ascribed to such trapped electron states. The interference of the impurity and the electron-phonon scattering mechanisms becomes most effective in this energy region. Here the electron is scattered by impurities, of which the potentials and transfer integrals are strongly changed during the scattering. This effect is important for the localization of electron states in the phonon field. In the structure-insensitive part of the main band (region of dominant hopping), the electron feels random modulations of the atomic and transfer energies, which are averaged out ($\sqrt{a}$ remains small compared with the effective half-band width).

The density of states ρ and the corresponding self-energy contributions σ_0, σ_1, σ_2 are compared in Fig. 5 (unsplit band) and Fig. 6 (split band) for alloys at several temperatures. The thermal disorder increases the absolute values of the imaginary parts of σ_0 and σ_2 ($\mathrm{Im}\sigma_0$, $\mathrm{Im}\sigma_2$ in Fig. 5(b) and (d), respectively); small changes appear in the imaginary part of σ_1 ($\mathrm{Im}\sigma_1$ in Fig. 5 (c)). Altogether, the thermal fluctuation cause an increase of the electron damping for all energies, as reflected by the imaginary part of the total self-energy. The "majority" and "minority" regions of the band (Fig. 5(a)) are stretched in the same manner with increasing temperature. These shifts in the spectrum are determined from the changes of the real parts of σ_0, σ_1, σ_2 ($\mathrm{Re}\sigma_0$, $\mathrm{Re}\sigma_1$, $\mathrm{Re}\sigma_2$ in Fig. 5(b),(c) and (d),respectively).

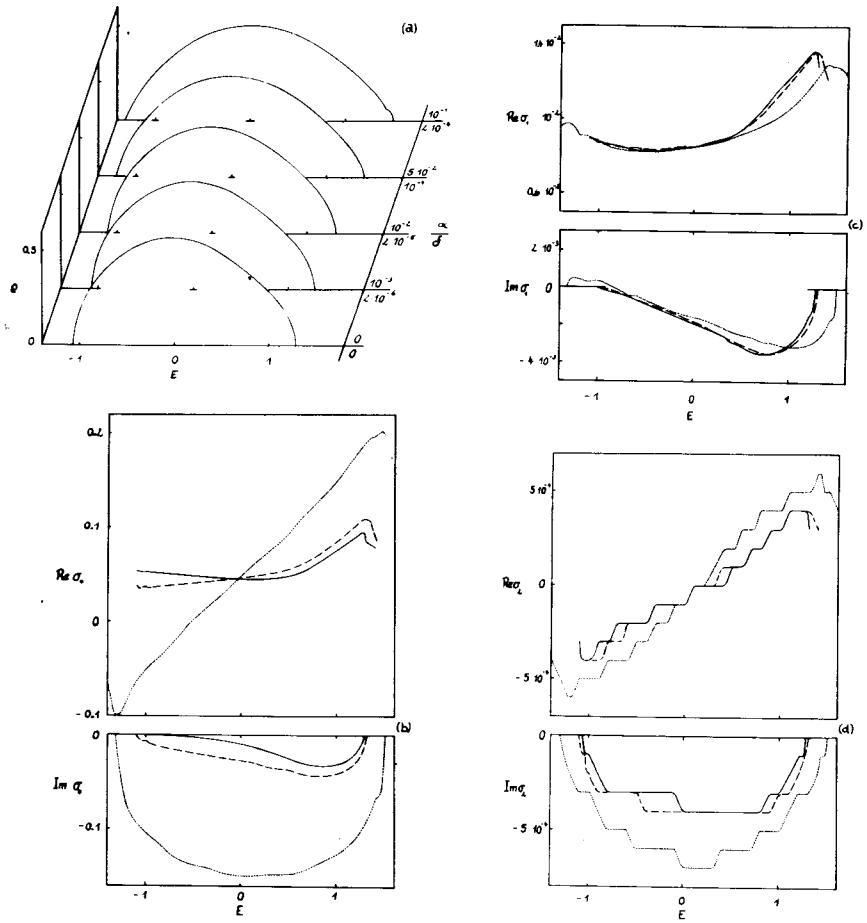

Fig. 5. Electronic density of states $\rho(E)$ (curves (a)) and real and imaginary parts of the self-energy contributions $\sigma_0(E)$, $\sigma_1(E)$, $\sigma_2(E)$ (curves (b),(c),(d),respectively) for an alloy with $c=0.3$, $\Delta_0=0.2$, $\Delta_1=0.4$ at several temperatures characterized by different values of (a,δ)-pairs. σ_0, σ_1, σ_2 are represented for $a=0,\delta=0$ (full lines), $a=10^{-2}$, $\delta=2\cdot10^{-5}$ (dashed lines), and $a=10^{-1}$, $\delta=2\cdot10^{-4}$ (dotted lines).

The imaginary parts of σ_0, σ_1, σ_2 concerning the split-band case (Fig. 6(b),(c), (d))have sharp peaks in the region of band deepening and near the band gap edges in the impurity part of the spectrum. These peaks indicate a strong damping of the electron states due to impurity scattering (especially in the static limit) and due to electron-phonon scattering (e.g., for $a = 10^{-1}$, $\delta = 8 \cdot 10^{-4}$). Moreover, the self-energy peaks for the imaginary parts are accompanied by precipitous changes in the real parts of σ_0, σ_1, σ_2. Such a change produces shifts in the spectrum. The variations of $\mathrm{Re}\sigma_0$, $\mathrm{Re}\sigma_1$, $\mathrm{Re}\sigma_2$ due to thermal fluctuations are reflected in a spreading of the band. As a consequence of thermal disorder, the absolute values of $\mathrm{Im}\sigma_0$, $\mathrm{Im}\sigma_1$, $\mathrm{Im}\sigma_2$ increase in wide regions of the bands, but can also decrease at energies of high damping (Fig. 6(b),(c)). In other words, the electron-phonon interaction leads to an

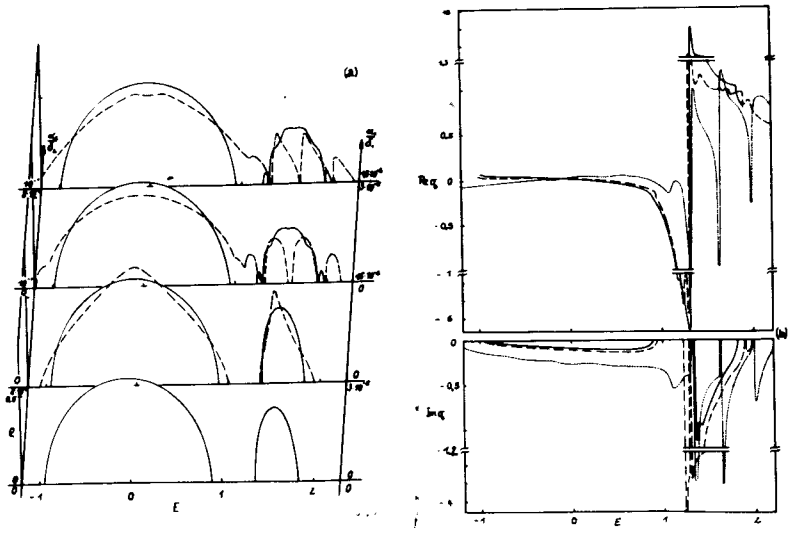

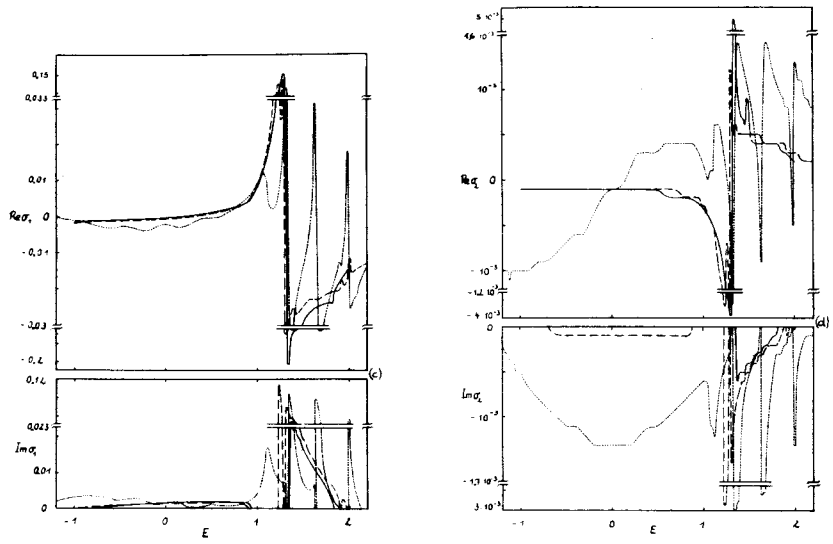

Fig. 6. Electronic density of states $\rho(E)$ and real and imaginary parts of the self-energy contributions $\sigma_0(E)$, $\sigma_1(E)$, $\sigma_2(E)$ for an alloy with $c = 0.15$, $\Delta_0 = 1.5$, $\Delta_1 = -0.4$ at different values of (a, δ)-pairs characterizing several temperatures. (a) ρ is shown for two different sets of parameter pairs (a_1, δ_1) (full lines) and (a_2, δ_2) (dashed lines). (b) σ_0, (c) σ_1, (d) σ_2 are plotted for $a = 0$, $\delta = 0$ (full lines), $a = 1.5 \cdot 10^{-2}$, $\delta = 3 \cdot 10^{-5}$ (dashed lines), and $a = 10^{-1}$, $\delta = 8 \cdot 10^{-4}$ (dotted lines).

additional scattering of the weakly and moderately damped electrons or can assist the hopping of the highly impurity-damped electrons. The reason for the peaked structure within the impurity subband (Fig.6(a)) is the same as discussed in connection with Fig. 4. Especially, the effect of the phonon-modulated transfer integrals on the density of states is discernible in Fig.6(a).

The dependence of $\rho(E)$ on the concentration c of A atoms is demonstrated in Fig. 7 for an alloy with parameters used in Fig.4 (d). The scattering strengths chosen here force to split off the impurity part of the main band. Further growth in c causes the height and width of the impurity subband to increase, whereas the host subband decreases. The sharp shape of $\rho(E)$ around the level ϵ^A indicates that the hopping from A atoms is reduced, i.e., an electron spends comparatively more time at A sites. The criterion for the appearance of structure in the minority band mentioned above is satisfied at low concentration (i.e., c= 0.1). Regarding this point, there may be localized states representing the trapping of electrons by potential fluctuations. Indeed, the electron-phonon interaction becomes more effective (compared to the impurity scattering) in a small-concentrated alloy.

In Fig. 8 we present the density of states in the general case where the electron-phonon interaction is affected by configurational disorder (compare with alloy parameters from Fig. 4(b)). This situation is expressed in terms of different thermal fluctuation parameters for the A and B com-

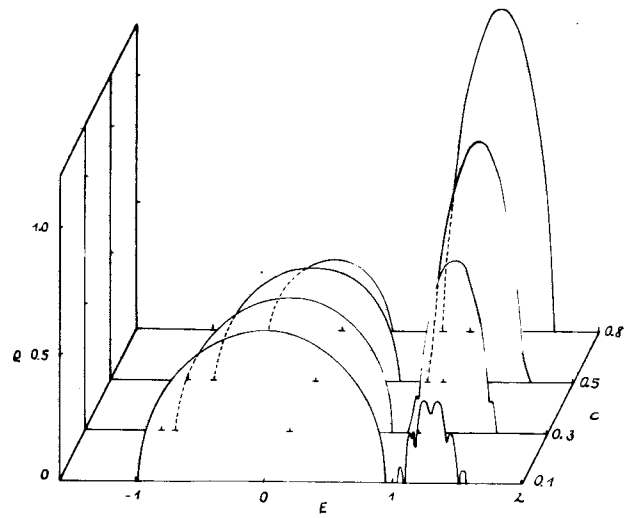

Fig. 7. Dependence of the electronic density of states $\rho(E)$ on the concentration c of A atoms in a binary alloy with $\Delta_0 = 1.2$, $\Delta_1 = -0.6$, $a = 10^{-2}$, $\delta = 2.10^{-5}$.

ponents. The qualitative picture of the split static-alloy band is preserved under the conditions $a^A < a^B$ and $\delta^A < \delta^B$. In the opposite case (i.e., $a^A > a^B$, $\delta^A > \delta^B$), dominant fluctuations of the scattering strengths for A atoms give rise to structure of $\rho(E)$ in the region of the impurity band. This part of the spectrum shows a behaviour similar to that obtained in Fig. 4; i.e., the minority-band density of states degenerates into a set of peaks. Note that this result is sensitively dependent on the thermal fluctuations of the transfer integrals. In the strongly-fluctuating case (i.e., $\delta^A = 10^{-3}$,

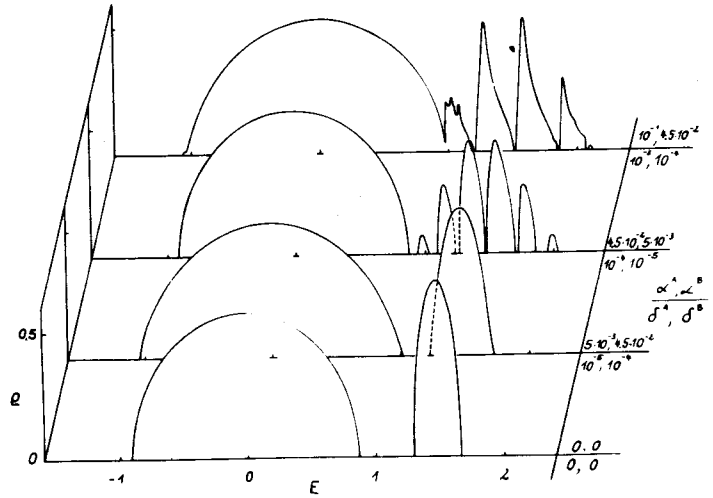

Fig. 8. Electronic density of states $\rho(E)$ in the case of different thermal fluctuation parameters for the A and B components. The curves represent an alloy with $c = 0.2$, $\Delta_0 = 1.4$, $\Delta_1 = -0.6$ at four temperatures characterized by $\alpha^A = \alpha^B = 0$, $\delta^A = \delta^B = 0$; $\alpha^B = 9\alpha^A$, $\delta^B = 10\delta^A$; $\alpha^A = 9\alpha^B$, $\delta^A = 10\delta^B$; and $\alpha^A \approx 2.2\alpha^B$, $\delta^A = 10\delta^B$.

$\delta^B = 10^{-4}$), considerably broadened spikes in $\rho(E)$ reflect the possibility of phonon-assisted hopping.

In this paper, our interest has centered around the problem of evaluating the electron energy spectrum. Another interesting question is associated with the nature of quantum states in the alloy system. The present model can be applied to study the electrical conductivity especially in connection with thermally-assisted hopping transport.

ACKNOWLEDGEMENTS

The authors are grateful to Th.Eifrig, A.Holas, and N.M.Plakida for useful discussions and valuable comments.

REFERENCES

1. E.Kolley and W.Kolley. JINR, E17-9353, Dubna, 1975.
2. A.B.Chen, G.Weisz and A.Sher. Phys.Rev., B5, 2897 (1972).
3. H.Fukuyama, H.Krakauer and L.Schwartz. Phys.Rev., B10, 1173 (1974).
4. Th.Eifrig, E.Kolley and W.Kolley. phys. stat.sol. (b), 67, 225 (1975).
5. B.Velický, S.Kirkpatrick and H.Ehrenreich. Phys.Rev., 175, 747 (1968).
6. Th.Eifrig. Dissertation KMU Leipzig, 1975.
7. A.B.Chen. Phys.Rev., B7, 2230 (1973).
8. M.Abramowitz and I.A.Stegun. Handbook of Mathematical Functions, Dover, New York, 1965.

Received by Publishing Department
on December 2, 1975.